

# Effect of Nozzle Diameter and Raster Angle on the Mechanical Properties of 3D Printed Nylon/Carbon Fibers

**Marwan A. Salman**

Department of Automated Manufacturing Engineering, Al-Khwarizmi College of Engineering, University of Baghdad, Iraq  
marwan@kecbu.uobaghdad.edu.iq (corresponding author)

**Sadoon R. Daham**

Department of Automated Manufacturing Engineering, Al-Khwarizmi College of Engineering, University of Baghdad, Iraq  
sadoon@kecbu.uobaghdad.edu.iq

**Wael H. A. Shaheen**

Department of Automated Manufacturing Engineering, Al-Khwarizmi College of Engineering, University of Baghdad, Iraq  
waelshaheen@kecbu.uobaghdad.edu.iq

**M. N. Mohammed**

Mechanical Engineering Department, College of Engineering, Gulf University, Sanad 26489, Bahrain  
dr.mohammed.alshekhly@gulfuniversity.edu.bh

**F. F. Mustafa**

Department of Automated Manufacturing Engineering, Al-Khwarizmi College of Engineering, University of Baghdad, Iraq  
dr.freiz@kecbu.uobaghdad.edu.iq

**Oday I. Abdullah**

Department of Energy Engineering, College of Engineering, University of Baghdad, Iraq | College of Engineering, Al-Naji University, Baghdad, Iraq | Department of Mechanics, Al-Farabi Kazakh National University, Kazakhstan  
oday.abdullah@tuhh.de

**S. Al-Zubaidi**

Department of Automated Manufacturing Engineering, Al-Khwarizmi College of Engineering, University of Baghdad, Iraq | Mechanical Engineering Department, College of Engineering, Gulf University, Sanad 26489, Bahrain  
salah.salman@kecbu.uobaghdad.edu.iq

Received: 19 December 2024 | Revised: 20 January 2025 | Accepted: 24 January 2025

Licensed under a CC-BY 4.0 license | Copyright (c) by the authors | DOI: <https://doi.org/10.48084/etasr.9979>

**ABSTRACT**

Fused Deposition Modeling (FDM) is classified as the most commonly used 3D printing process due to its low cost, wide range of material selection, and high accuracy. As an additive manufacturing method, FDM selectively deposits a melted plastic material layer by layer to produce a 3D object according to a geometry defined by a CAD model. The 3D printing process parameters, including infill density, printing speed, and

printing orientation, have a huge effect on the mechanical properties of the 3D printed parts. Thus, finding the optimum 3D printing parameters is a very significant task that enriches the FDM 3D printing process, resulting in 3D printed parts with augmented mechanical performance. The present study investigates the effects of the FDM injector's nozzle diameter and printing path direction (raster angle) on the mechanical properties of the nylon/carbon fiber composite 3D printed parts. The two targeted parameters are optimized through experimental tests on the elastic and flexural strength. Their impact on the nylon/carbon fiber composites' microstructure is also explored deploying Scanning Electron Microscopy (SEM). The findings provide a comprehensive understanding of the mechanical performance of nylon/carbon fiber composite 3D printed parts. In addition, inspecting the internal microstructure of the materials, especially at the interface zone between the nylon and carbon fiber, provides an explanation of the material composites' failure mechanism under various loads.

*Keywords-fused deposition modeling; raster angle; nylon/carbon fiber; 3D printing; flexural bending*

## I. INTRODUCTION

The manufacturing industry has recently developed through the progress of 3D printing, which encourages the production of complex high-precision geometries. Among the various 3D printing technologies, FDM came to the fore due to its reliability and high precision. Carbon fiber composites are introduced as a powerful addition to the materials used in the FDM method without affecting the 3D printing process. Based on this fact, nylon/carbon fiber composites have garnered substantial attention because of their exceptional mechanical properties, such as improved strength, stiffness, and lightweight attributes. In the 3D printing framework, the mechanical properties of the final product are highly affected by printing parameters, such as print speed, print orientation infill density, and nozzle diameter. Hence, understanding the effect of various printing parameters on the mechanical performance of nylon/carbon fiber composites is critical for optimizing the proportion of the final 3D printed product and increasing its use in extended high-performance applications. Many researchers have taken these material composites into consideration. Authors in [1] studied the effect of 3D printing parameters, involving printing temperature, printing speed, side step, and layer thickness, on the mechanical properties of 3D printed nylon PAG/carbon fiber composites. The study focused on the combined effect of the post-processing pressure and temperature on the internal voids of the 3D printed product. Authors in [2] explored the influence of carbon fiber weight fraction on the mechanical properties of nylon PAC/PAG/carbon fiber composites. The study concluded that the 3D printed samples with 20% carbon fibers exhibited a significant improvement in impact strength, namely a 500% increase, and a 50% increase in the shear strength. In contrast, authors in [3] prepared various types of prepreg continuous carbon fiber filaments for the 3D printing of the samples. According to the results, the resin content and infiltrate degree had an obvious effect on the tensile and shear strength of the 3D printed nylon 6/ carbon fiber composites. Authors in [4] investigated the 3D printing orientation impact on the mechanical properties of nylon/carbon fiber composites. The findings revealed that the specimens printed with horizontal orientation exhibited superior mechanical performance compared to those printed utilizing other orientations. Other studies have focused on using hybrid continuous fibers as reinforcement agents with nylon matrix. For instance, authors in [5] used the FDM 3D printing method to prepare a combination of continuous carbon and Kevlar fibers with a

nylon matrix. The research investigated the influence of the hybrid configurations, raster orientation, and stacking sequences on the failure behavior of the composites. Authors in [6] studied the effect of short carbon fibers on the mechanical properties of the 3D printed nylon PAG. Various properties were included, like electrical conductivity and piezoresistivity. The results demonstrated that the addition of short carbon fibers improves the tensile and impact strength. Similarly, authors in [7] explored the mechanical properties of the laminated carbon Fiber Reinforced Polymer (FRP), which is made by integrating both continuous and chopped carbon fibers into the thermoplastic matrix. Notable improvements in energy absorption and impact strength were demonstrated. Authors in [8] examined the nylon PAG/carbon fiber composite material to display the impact of 3D printing direction, infill density, and thermal stresses, which arise during the 3D printing process, on the mechanical properties of the 3D printed specimens. The study concluded that the 3D printing direction (raster angle) significantly affects the tensile strength and hardness of the material. Multiple studies have focused on the 3D printed nylon/carbon fiber composites and their mechanical properties, namely tensile strength, bending strength, impact strength, with the detailed mechanical characteristics that describe material performance outlined in [9-14]. The aforementioned studies have investigated the main parameters of the FDM process. However, there has been a restricted focus on the combined effects of the nozzle diameter and raster angle on the microstructure and mechanical properties of the 3D printed products, which has generated a stringent gap in the industrial application knowledge. The present work provides a thorough understanding of the combined effects of the studied parameters on the nylon/carbon fiber composite mechanical properties, which is not extensively included in the current literature. Furthermore, it presents an experimental framework for these properties' direct effect on the tensile and flexural strength of the final printed materials, while feasible recommendations for adjusting the FDM setting to specific material requirements are also provided.

## II. MATERIAL DEFINITION

The materials utilized in this study are manufactured by the Fillamentum additive polymer company [15]. Nylon CF-15 consists of nylon polymer as a base (matrix) material and carbon fibers as an additive reinforcement. The carbon fibers are milled and are 100  $\mu\text{m}$  long. The material composites are produced as a filament, with 600 g weight and a density of 1.08  $\text{g/cm}^3$ . The materials are designated to have a tensile strength of

54.5 MPa with 103 % elongation at break and 500 MPa as a tensile modulus. They additionally have a Charpy impact resistance of 86.2 kJ/m<sup>2</sup>, hardness of 75, and melting temperature of 160°C.

### III. FDM 3D PRINTING PROCESS

FDM 3D printing is introduced as the most precise manufacturing process, especially for polymer composites. In addition to its precision, it has great reliability and repeatability, rendering it very easy to operate. The Comgrow Creality Ender 6 3D printer [16] was employed to print the material at a temperature of 240°C with a preheated pad at 90°C. The particular printer is selected because it provides a thermally isolated environment around the printing zone. Such isolation is very important to prevent changes in ambient temperature during the 3D printing process. Furthermore, a 3DLAC adhesive stick is used to affix the specimen with the 3D printer bed to avoid the print bowing out (elephant's foot), as depicted in Figure 1.

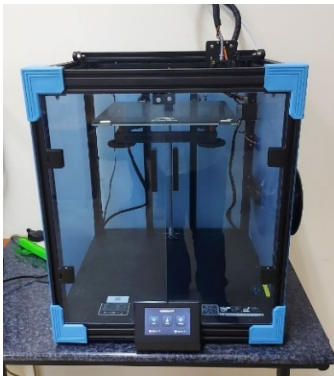


Fig. 1. Comgrow Creality Ender 6 3D printer.

Two problems emerge due to the milled carbon fiber existence. First, the filament dimensions are guaranteed within the tolerance  $\pm 0.10$  mm, signifying that there is a variation in the printed line cross-section. Such a variation affects the adhesion strength between layers. Secondly, the abrasive properties of the carbon fibers lead to fast nozzle wear, especially for brass nozzles. Thus, the nozzle of the 3D printer must be changed every three specimens to ensure a uniform and smooth printing process. For both tensile and bending tests, five raster angles were selected to be tested, namely, 0°, 15°, 45°, 75°, and 90°. Furthermore, three different nozzle diameters were used to manufacture the specimen, 0.4, 0.6, and 0.8 mm. The settings of the 3D printing process have a considerable influence on the mechanical properties of the produced specimen. As a result, several parameters were set to meet the material's requirements, as listed in Table I.

TABLE I. 3D PRINTING PARAMETERS

Printing parameters	Value
Infill (raster) pattern	lines
Layer thickness	0.28 mm
Printing speed	20 mm/s
Nozzle temperature	240 °C
Bed temperature	90 °C
Infill density	100%

### IV. EXPERIMENTAL METHODS

In the tensile test experiment, the produced specimens were designed to be pulled for a finite deformation under controlled parameters to investigate their mechanical properties, i.e. Young's modulus, elongation, and tensile strength. In addition, the specimens must be prepared carefully to collect indicative data from the tensile experiments. Thus, many aspects, like print settings and printing orientation, were considered. Appropriate testing standards were adopted during the 3D printed specimen preparation process. In many instances of plastic specimen tensile tests, the ASTM D638 [17] standards, which have established various specimen shapes, were employed to delineate the specimen dimensions and geometry. The dog-bone shape is the most common shape used in tensile tests because it provides a uniform distribution of the stress during the test. Furthermore, it tapers at both ends to accommodate the holds of the testing machine. Figure 2 portrays the standard specimen dimensions as well as the raster angle. For every nozzle diameter and raster angle, five specimens are prepared according to the ASTM D638 standards. A testometric testing machine [21] was employed, and grips were utilized to hold the specimen during the test. Furthermore, the testing machine has the ability to gauge both force and resulting elongation. Commonly, an extensometer is utilized to measure elongation, and a load cell to estimate force. It is worth mentioning that the specimen is aligned in the machine gripper carefully to prevent any bending or torsion, leading to more accurate results. Moreover, the experiment is applied at room temperature with a deformation speed of 1 mm/min according to the ASTM D638 standards.

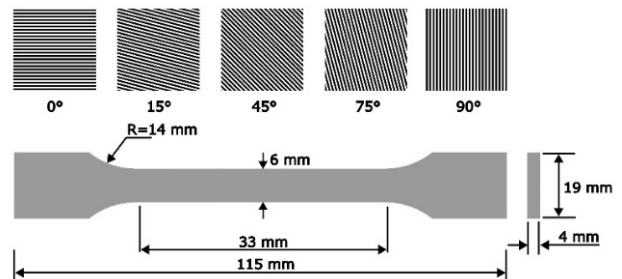


Fig. 2. Dimensions of the tensile specimen and raster angles.

The specimen was pulled apart until failure occurred. During this process, the test machine records the force and elongation applied to the specimen. The main objective behind this test is to estimate the stress-strain curves. According to ASTM D638 standards, the stress is calculated by:

$$\sigma = \frac{F}{WT} \quad (1)$$

where  $\sigma$  represents the tensile stress (N/mm<sup>2</sup>),  $F$  is the calculated force (N),  $W$  is the specimen width (mm), and  $T$  is the specimen thickness (mm).

Several measured values can be evaluated from the stress-strain curve, namely, tensile strength, Young's modulus, and stress at break. Ultimately, a sample of the prepared 3D printed specimens of the tensile test is presented in Figure 3.



Fig. 3. Dimensions of the tensile specimen and raster angles.

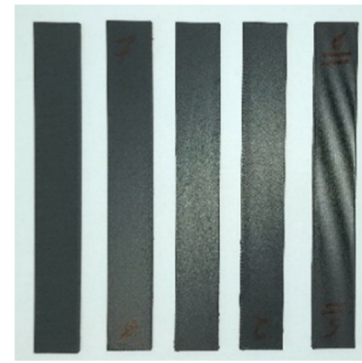


Fig. 5. Sample of bending test specimens.

In the bending test, all the prepared specimens were tested under the ASTM D 7264 standard test method for the flexural properties of polymer matrix composite materials to be estimated [17]. For every diameter and raster angle, five specimens were prepared according to the dimensions shown in Figure 4.

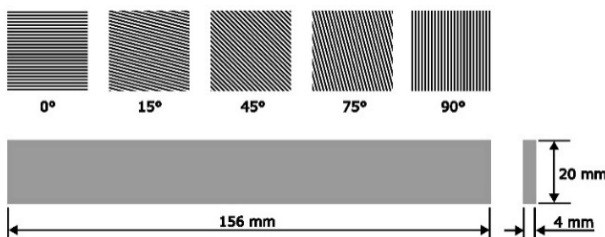


Fig. 4. Representation of the flexural specimen geometry and raster angles.

A testometric flexural testing machine was used to investigate the specimen performance under a bending load. The specimen was supported on both ends and a perpendicular load was applied to the midpoint of the upper base of the specimen at a 3 mm/min speed. The applied deformation curvatures to the specimen cause deflection at the midpoint, and the deflection was documented concurrently. All 75 specimens were tested at the same strain rate and at room temperature, to estimate their maximum flexural stress, rupture flexural stress, flexural bending modulus, and stress-deflection curve.

Scanning Electron Microscopy (SEM) images provide an effective tool for investigating the microstructure of the 3D printed material composites. With high magnification, very significant details regarding the material's microstructure can be revealed. Furthermore, an important clarification can be estimated about the failure mechanism that eventuates under stress, which can be determined and the results can be collected through SEM. The Inspect TM F50 SEM scanner was employed to explore the microstructure details of the nylon CF-15 composite at the cross-section area of the failure zone. The scanner is easy to use and provides high-resolution images with a stable platform.

## V. RESULTS AND DISCUSSION

The tensile tests were performed on three sets of nylon CF-15 3D printed specimens with a different nozzle diameter for each set, 0.4 mm, 0.6 mm, and 0.8 mm. Every set consisted of five subsets with varying raster angles, namely, 0°, 15°, 45°, 75°, and 90°. Moreover, every subset contains five specimens. All 75 specimens were pulled in the test machine under a constant deformation rate of 1 mm/min at room temperature. The resulting stress-strain curves are illustrated in Figure 6.

The tensile strength of each nozzle diameter and raster angle is displayed in Figure 7. Before analyzing the behavior of the material under tensile loads, the 3D printed specimens were inspected by a microscope to take a shot of the material composite microstructure after the 3D printing process, which is showcased in Figure 8. As observed by the resulting picture, the carbon fiber alignment with the printing direction has been proven. The estimated stress-strain curves demonstrate various materials' behavior, explaining the combined influence of the studied 3D printing parameters, nozzle diameter and raster angle. The 3D printed materials exhibit a lower tensile strength with a relative elastic behavior till failure for a lower nozzle diameter (0.4 mm). Furthermore, the materials take a lower strain to failure, which indicates a clear brittle performance of the 3D printed materials. Widening the nozzle diameter leads to much higher tensile strength with a noticeably higher strain to failure, meaning that the materials exhibit greater ductile behavior under tensile loads. In addition, a markable elastic-plastic deformation is experienced by the 3D materials, signifying a wider necking region in the tensile test.

Due to the thinner extruded line width, the bigger diameter of the nozzle can fill the volume space of the printed specimen by depositing extra molten material during the 3D printing process. Therefore, the microstructure of the 3D printed specimen has a much lower volume of voids formed between the layers during the 3D printing process. As a consequence, the specimens produced with higher nozzle diameters experience higher tensile strength. Moreover, the reduction of the void volume inside the material microstructure enhances material ductility and leads to a relatively longer necking region.

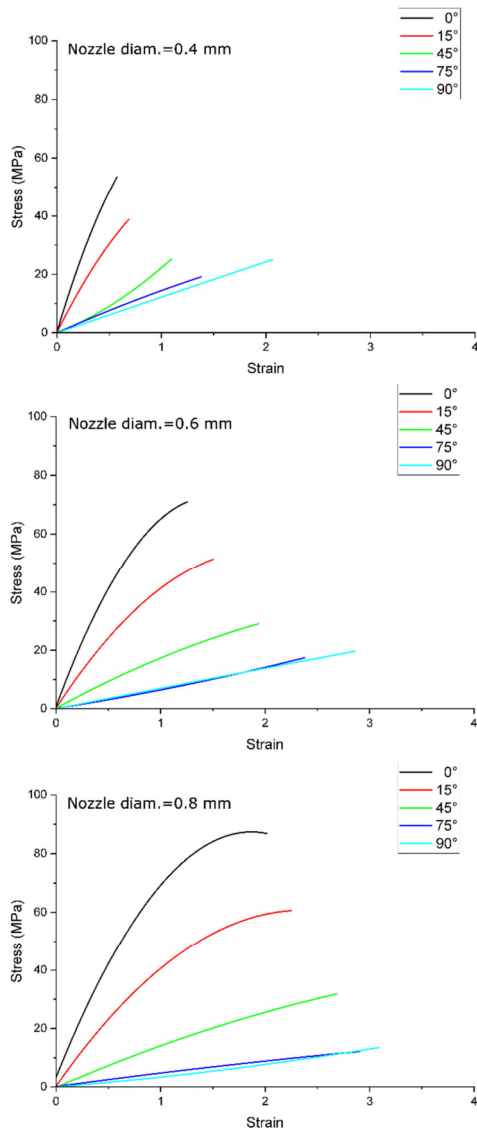


Fig. 6. Tensile test results of each nozzle diameter and raster angle.

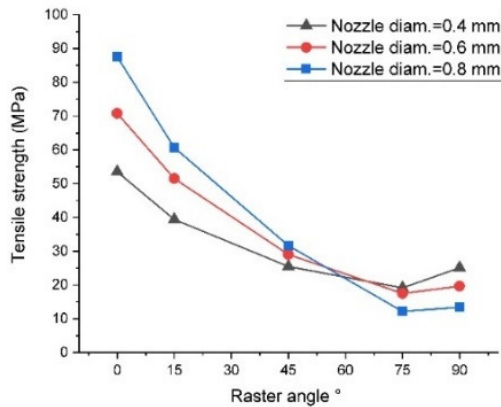


Fig. 7. Effect of raster angle on tensile strength of each nozzle diameter.

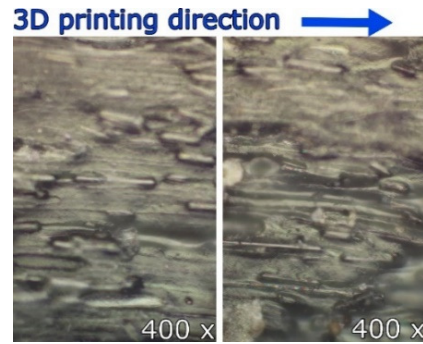


Fig. 8. Carbon fiber alignment with respect to printing direction.

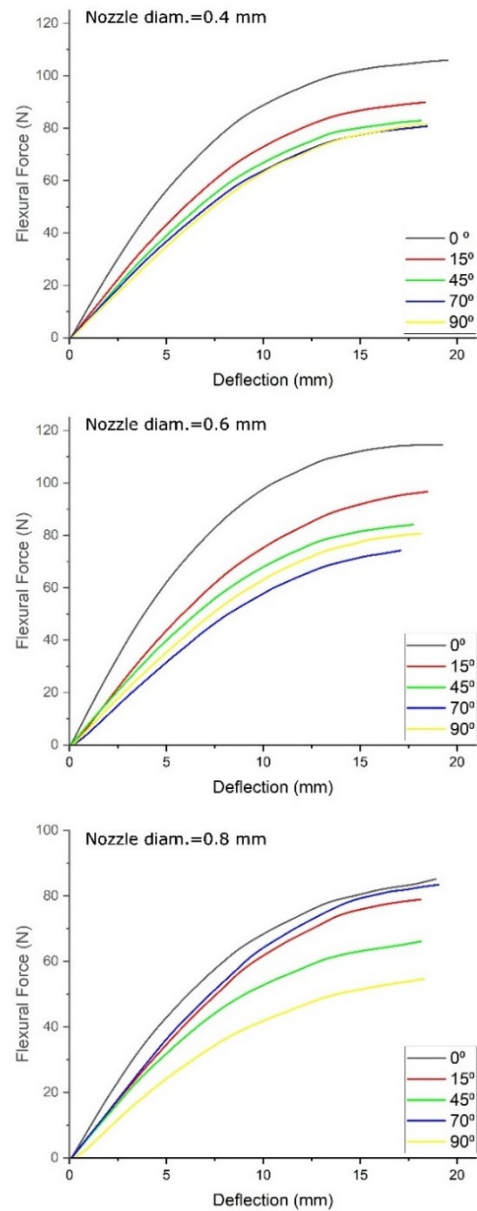


Fig. 9. Flexural force-deflection curves of each nozzle diameter and raster angle.

The second point is the fact that the print path orientation distributes the external tensile load between the extruded line itself and the adhesive force between the extruded lines. In other words, in specimens with a  $0^\circ$  raster angle, the external tensile load is resisted by the extruded lines of nylon CF-15 composite because they are parallel to the loading direction. In the specimen of  $90^\circ$  raster angle, the adhesion between the extruder lines controls the material behavior during the tensile test. All raster angles between  $0^\circ$  and  $90^\circ$  show a combination of the aforementioned properties. It should be noted that the print path orientation parallel to the tensile load ( $0^\circ$  raster angle) gives the extruded lines a chance to show the plastic nature of nylon CF-15, which is represented by the nonlinear stress-strain curves. Furthermore, a specimen of print path orientation fully perpendicular to the loading direction ( $90^\circ$  raster angle) demonstrates more gradual dislocations between the extruded lines, which give the material greater ductility with a noticeable reduction in the tensile strength during the tensile test. In the bending test, a total of 75 specimens were tested, five specimens for every raster angle and nozzle diameter. Furthermore, three-point bending test was implemented by applying a total force at the midspan, and the resulting total deflection at the same point was recorded. The resulting flexural force-deflection curves are depicted in Figure 9. For a clearer and more understandable representation of the results, the flexural strength of the tested specimen is compared with the raster angles, as can be seen in Figure 10.

It is observed that the specimens produced with a 0.6 mm nozzle diameter have higher performance against the bending force than the other specimens. Furthermore, the specimens made with a 0.8 mm nozzle diameter show a lower response to the flexural test. There are three main factors controlling the material's performance during the bonding test. The first is the adhesion force between the printed layers. Specimens with low nozzle diameters will have significantly finer print lines and a thinner layer thickness. This will lead to a higher adhesion strength between layers and higher flexural strength for a constant raster angle. The second factor is the microstructure of the 3D printed materials, which is highly affected by the nozzle diameter.

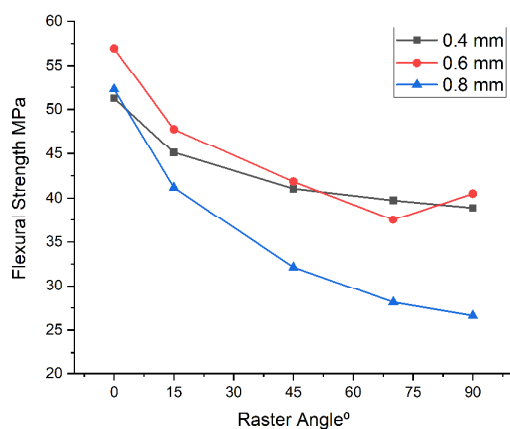


Fig. 10. Effect of raster angle on the flexural strength.

Specifically, a 0.8 mm nozzle diameter provides more material during the 3D printing process, reduces the volume of the voids between layers, and builds a stronger microstructure. Therefore, the produced specimens have better performance. The carbon fiber's alignment with the loading direction is the third factor, which plays a substantial role in the bending test. This factor is controlled by the raster angle used during the 3D printing process. Therefore, for a constant nozzle diameter, the flexural strength of the 3D printed nylon CF-15 specimen is increased at a raster angle of  $0^\circ$  and reduced to the minimum at a raster angle of  $90^\circ$ . Keeping in mind these factors, the specimens of 0.6 mm nozzle diameter are considered a mix of the interlayer adhesion strength and low void volume microstructure. Accordingly, they exhibit the best flexural strength at all raster angles compared to the specimens with other nozzle diameters.

By focusing on the cross-section area of the failure zone of 3D printed specimens, essential features turn apparent using SEM images. Furthermore, distinctive matrix material, carbon fibers, and the interface between them can be recognized. Being a highly powerful tool, SEM offers detailed inspections detecting the fracture surface characteristics at the microscale level. Two SEM images were taken and magnified two times (1000x, 2000x) for the cross-section of the failure zone, as illustrated in Figure 11.

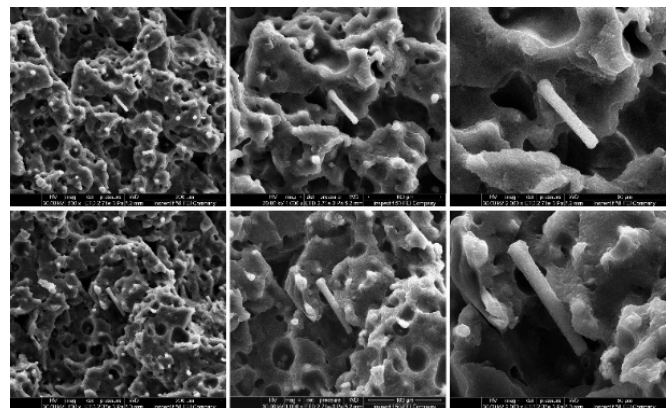


Fig. 11. SEM images of the specimen at the failure zone.

SEM images demonstrate the failure mode of the microscale level. The adhesion strength between the matrix materials and the carbon fibers is a crucial attribute of the material's composite performance. If the adhesion strength is relatively high, the carbon fibers have the ability to transfer loads to the nylon matrix effectively, improving material performance under stress. On the contrary, the carbon fibers are pulled out of the nylon matrix in the case of imperfect bonding, leading to weak material performance. The SEM images show areas where carbon fibers are debonding from the nylon matrix at the failure zone. However, the debonding occurs due to gaps or voids between the carbon fibers and the surrounding matrix. These gaps and voids are formed during the 3D printing process due to high temperature and high-speed printing. In addition, the pulled-out carbon fibers leave behind rough surfaces and voids on the fractured cross-section area. The

explored failure mechanism is common in the behavior of the material composite that has weak matrix-fiber adhesion, greatly affecting the 3D printed nylon CF-15 composite's mechanical properties.

## VI. CONCLUSIONS

The 3D printing parameters significantly influence the mechanical properties of 3D printed nylon/carbon fiber composites. Specifically, the nozzle diameter and raster angle affect the internal bonding between the nylon matrix and carbon fibers, microstructure, and overall performance of the material under load. Three sets of specimens with three different nozzle diameters, namely 0.4 mm, 0.6 mm, and 0.8 mm underwent a tensile test. The findings indicate that there is a clear nozzle diameter impact on material performance under tensile load. In specific, the specimens of 0.8 mm nozzle diameter exhibit maximum tensile strength compared to those having other nozzle diameters. Furthermore, five sets of specimens printed with five raster angles of 0°, 15°, 45°, 75°, and 90°, were tested for every nozzle diameter under tensile load to investigate the printing direction effects on material behavior. The results indicate that the specimens printed with a direction parallel to the applied tensile load (raster angle = 0°) have higher tensile strength than those with other raster angles. Increasing the raster angle leads to a notable decrease in material performance under tensile load.

In the same context, the mechanical performance of nylon/carbon fiber composites is explored under flexural banding load. Three nozzle diameters, 0.4 mm, 0.6 mm, and 0.8 mm, were employed to print three sets of specimens. The obtained results exhibit that the specimens of 0.6 mm nozzle diameter achieved the best performance under banding load because they offer a balance between the void volume ratio caused by the nozzle diameter and adhesion strength between the printed layers. In summary, the 3D printing parameters, nozzle diameter, and raster angle play a great part in specifying the mechanical performance of 3D printed nylon/carbon fiber composites. In addition, the studied parameters have a significant effect on material microstructure, especially at the interface zone between the carbon fiber and nylon matrix, providing a deep understanding of the material nature as well as the failure mechanism under various loads. The optimization of the targeted 3D printing parameters is crucial for reaching the best material performance regarding tensile and flexural strength. The findings of the present work increase the ability of designers and engineers to optimize the 3D printed products by fine-adjusting the nozzle diameter and raster angles, resulting in optimum mechanical performance. Furthermore, the results offer a deep understanding of the relationship among the printing orientation, mechanical behavior, and material flow, contributing to the additive manufacturing field. It can be concluded that the proposed approach inspires further research on the combined effects of Fused Deposition Modeling (FDM) parameters, such as layer thickness, infill density, and material type, establishing pathways for FDM process design optimization.

## REFERENCES

- [1] S. Chen, L. Cai, Y. Duan, X. Jing, C. Zhang, and F. Xie, "Performance enhancement of 3D-printed carbon fiber-reinforced nylon 6 composites," *Polymer Composites*, vol. 45, no. 6, pp. 5754–5772, 2024, <https://doi.org/10.1002/pc.28161>.
- [2] N. A. Mohd Radzuan, N. N. Khalid, F. M. Foudzi, N. R. Rajendran Royan, and A. B. Sulong, "Mechanical Analysis of 3D Printed Polyamide Composites under Different Filler Loadings," *Polymers*, vol. 15, no. 8, Jan. 2023, Art. no. 1846, <https://doi.org/10.3390/polym15081846>.
- [3] Y. Zhuang, B. Zou, S. Ding, X. Wang, J. Liu, and L. Li, "Preparation of pre-impregnated continuous carbon fiber reinforced nylon6 filaments and the mechanical properties of 3D printed composites," *Materials Today Communications*, vol. 35, Jun. 2023, Art. no. 106163, <https://doi.org/10.1016/j.mtcomm.2023.106163>.
- [4] I. M. Alarif, "Investigation of the dynamic mechanical analysis and mechanical response of 3D printed nylon carbon fiber composites with different build orientation," *Polymer Composites*, vol. 43, no. 8, pp. 5353–5363, 2022, <https://doi.org/10.1002/pc.26838>.
- [5] S. Li, K. Wang, W. Zhu, Y. Peng, S. Ahzi, and F. Chinesta, "Investigation on the mechanical properties of 3D printed hybrid continuous fiber-filled composite considering influence of interfaces," *The International Journal of Advanced Manufacturing Technology*, vol. 123, no. 9, pp. 3147–3158, Dec. 2022, <https://doi.org/10.1007/s00170-022-10398-7>.
- [6] S. Dul, L. Fambri, and A. Pegoretti, "High-Performance Polyamide/Carbon Fiber Composites for Fused Filament Fabrication: Mechanical and Functional Performances," *Journal of Materials Engineering and Performance*, vol. 30, no. 7, pp. 5066–5085, Jul. 2021, <https://doi.org/10.1007/s11665-021-05635-1>.
- [7] Y. Delporte and H. Ghasemnejad, "Manufacturing of 3D Printed Laminated Carbon Fibre Reinforced Nylon Composites: Impact Mechanics," *Open Journal of Composite Materials*, vol. 11, no. 1, pp. 1–11, Dec. 2020, <https://doi.org/10.4236/ojcm.2021.111001>.
- [8] F. Calignano, M. Lorusso, I. Roppolo, and P. Minetola, "Investigation of the Mechanical Properties of a Carbon Fibre-Reinforced Nylon Filament for 3D Printing," *Machines*, vol. 8, no. 3, Sep. 2020, Art. no. 52, <https://doi.org/10.3390/machines8030052>.
- [9] X. Li *et al.*, "High strength carbon-fiber reinforced polyamide 6 composites additively manufactured by screw-based extrusion," *Composites Science and Technology*, vol. 229, Oct. 2022, Art. no. 109707, <https://doi.org/10.1016/j.compscitech.2022.109707>.
- [10] T. Liu, X. Tian, Y. Zhang, Y. Cao, and D. Li, "High-pressure interfacial impregnation by micro-screw in-situ extrusion for 3D printed continuous carbon fiber reinforced nylon composites," *Composites Part A: Applied Science and Manufacturing*, vol. 130, Mar. 2020, Art. no. 105770, <https://doi.org/10.1016/j.compositesa.2020.105770>.
- [11] W. Chen *et al.*, "Additive manufacturing of high-strength polyamide 6 composites reinforced with continuous carbon fiber prepreg," *Polymer Composites*, vol. 45, no. 1, pp. 668–679, 2024, <https://doi.org/10.1002/pc.27805>.
- [12] T. Lan, L. C. Dong, Z. Lu, S. F. Guo, H. Zhang, and Y. C. Pei, "Influence of Layer Thickness and Continuous Carbon Fiber on the Mechanical Property of 3D Printed Polyamide," *Key Engineering Materials*, vol. 861, pp. 165–169, 2020, <https://doi.org/10.4028/www.scientific.net/KEM.861.165>.
- [13] A. Hisham, S. Ali, S. Abdallah, A. N. A. Mohammed, R. A. Susantyoko, and S. Pervaiz, "Experimental and Statistical Optimization of Carbon-Fiber Reinforced Nylon Composite Based 3D Printed Cellular Structures," in *International Mechanical Engineering Congress and Exposition*, Columbus, OH, USA, Nov. 2022, <https://doi.org/10.1115/IMECE2022-95727>.
- [14] N. Askarizadeh and M. R. Mohammadzadeh, "Numerical Analysis of Carbon Fiber Reinforced Plastic (CFRP) Shear Walls and Steel Strips under Cyclic Loads Using Finite Element Method," *Engineering, Technology & Applied Science Research*, vol. 7, no. 6, pp. 2147–2155, Dec. 2017, <https://doi.org/10.48084/etasr.1279>.
- [15] "Fillamentum | addi(c)tive polymers." <https://fillamentum.com/>.

- [16] "Crealty - Official Website." <https://www.crealty.com/>.
- [17] *ASTM D7264/D7264M-07(2007), Standard Test Method for Flexural Properties of Polymer Matrix Composite Materials.* West Conshohocken, PA, USA: ASTM International, 2007.
- [18] "Meiji Techno - Quality Microscopes." <https://meijitechno.co.uk/>.